INFLUENCE OF SLAB ON THE SEISMIC RESPONSE OF SUB-STANDARD DETAILED EXTERIOR REINFORCED CONCRETE BEAM COLUMN JOINTS

W.Y.Kam[1], P. Quintana Gallo[1], U. Akguzel[1], S. Pampanin[2]

ABSTRACT

For the seismic performance assessment of existing sub-standard detailed exterior beam-column joints, it is critical to accurately establish the hierarchy of strength of each element and therefore the likely failure mechanism. However, in current practice, the influence of cast-in-situ slab and transverse beams is typically neglected or calculated based on equations that were derived from modern detailed beam-column joint subassembly tests. In literature, experimental studies for non-ductile beam-column joints constructed prior to the 1970s, thus before the introduction of capacity design principles, explicitly considering the influence of slabs are scarce. This paper presents the experimental results of comprehensively instrumented four 2/3-scaled one-way (two-dimensional, 2D) and two-way (three-dimensional, 3D) exterior beam-column joints with and without slabs. Tests were conducted under uni-directional and bi-directional quasi-static lateral loading with concurrent varying axial loading. Comparison in terms of global and local behavior between specimens show the influence of the floor slab and the transverse beam in the resistance mechanism of the beam-column-joint subassembly elements in different ways, depending on the type of frame and the loading protocol. Preliminary recommendations for assessment are tentatively provided as closure.

Introduction

Recent experiences with devastating earthquakes as well as research findings have confirmed the vulnerability of non-ductile reinforced concrete (RC) buildings, designed according to old building codes (NZS95:1955, 1955, ACI318-63, 1963). This leads to the urgent need for a methodic evaluation of the seismic vulnerability of the existing building stock as a starting point (diagnosis) for the design of adequate retrofit interventions. The (relatively) limited information and knowledge on the expected seismic actions on one hand and the lack of capacity design philosophy, developed in the mid-late 1960s, and the use of non-ductile detailing (i.e. use of plain round bars, 180° end hooks into joint, lap splices in potential plastic hinge zones, no joint transverse reinforcement) on the other hand, have been widely recognized as the main deficiencies of such structures (Beres et al, 1996, Pampanin et al, 2002, Park, 2002).

In the past, research has been done on RC beam-column (b-c) joint subassemblies with

[1]Ph.D. Candidate, Department of Civil and Natural Resources Engineering, University of Canterbury, Christchurch, New Zealand.
[2]Associate Professor, Department of Civil and Natural Resources Engineering, University of Canterbury, Christchurch, New Zealand.

floor slabs in order to establish the proper seismic design procedures for b-c joints under a jointed US-Japan-NZ research programme (French et al, 1991). The experiments funded by this large research programme included various interior an exterior b-c joints, under either uni- or bi-directional lateral loading, with and without floors slabs and designed to various national seismic codes (US, Japan, NZ etc). Concurrently, several researchers have tested b-c subassemblies in order to understand the mechanics of the joint including the slab and the intension of modifying the normative to account for that effect (Ehsani et al, 1985, Durrani et al, 1987, Cheung et al, 1991, Di Franco et al, 1995). Within a research project focused on developing seismic retrofit solutions, several 1/3-scaled benchmark b-c joints with floor slabs subassemblies have been tested (Aycardi et al, 1994) in order to assess the seismic vulnerabilities of gravity-designed RC frames. However, the research did not put much attention in developing the necessary modification to existing assessment procedures and equations

This research presents further experimental data with regard to quasi-static tests on four 2/3-scaled one-way and two-way exterior b-c joints with and without slabs tests under uni-directional and bi-directional lateral loading and varying axial loading – designed to study the influence of floor slab on such types of b-c-joints. Specifically, the influence of slabs on one-way and two-way b-c joints are discussed with preliminary assessment suggestions for non-ductile joints are presented as closure.

Research Significance

The current seismic evaluation of the capacity of non-ductile b-c joints with floor slabs is based on few assumptions such as effective width equations that were derived from experimental tests on b-c joints designed to modern seismic codes. This is likely to be un-conservative in the assessment of the hierarchy of strength of these pre-1970s b-c joints, in particularly where realistic slab participation generally amplifies the beam negative moment capacity but might potentially violate the capacity design requirements for strong-column weak-beam. Furthermore, the presence of transverse (spandrel) beam on non-ductile b-c joints with no joint shear reinforcement and plain-round reinforcement bars might lead to interesting outcomes, which are currently untested. In addition, the effectiveness of slab participation within a bi-axially loaded corner b-c joint under varying axial load, more proper representing the actual loading condition within a frame system, is also something previously untested. Therefore, the experiment program of this research aim to reflect the unique contribution of these as-built configurations with floor slabs when subjected to more advanced loading protocol. The test results provided some indications for upper- and lower-bound equations to account for slab-participation.

Experimental Program

Specimen description

Two two-dimensional (2D) and two three-dimensional (3D) 2/3 scaled exterior b-c joint subassemblies representative of pre-1970s construction practice (i.e. plain round with 180 deg. standard end hook anchorage and absence of transverse reinforcement in the joint) were tested. All specimens detailed and designed according to typical older construction practice via meeting the requirements of older building codes (NZS95:1955, , ACI318-63)

The benchmark test specimens represented an exterior joint of an interior frame (2D-B)

and a corner joint (3D-B) of a typical mid-rise residential building. Each type of joint was also constructed and tested with floor slab (i.e., 2D-S for two-dimensional and 3D-S for three-dimensional). The cast-in-situ slab had thickness of 100mm with R6 mesh on 150mm square and cantilevered length of 490mm from beam center-line. The reinforcement detailing of the slab onto the b-c joint was consistent with typical gravity-designed one-way slab, with continuous or tension anchorage for top mesh bars, and discontinued or hooked bottom mesh bars. The transverse beam stub adopted the same reinforcing detailing as the main beam, not an uncommon assumption in pre-1970s construction.

Geometry and reinforcement detail of the test units are shown in Figure 1. All test units had 230mm x 230mm columns and 330mm deep x 230mm wide beams. Same steel reinforcement configuration was used in both x- and y-directions of 3D specimens. The average values of yield stress, f_y, for the smooth mild longitudinal and transverse reinforcement are 350MPa and 425MPa, respectively. The values for concrete compressive strength at the day of testing are given in Table 1.

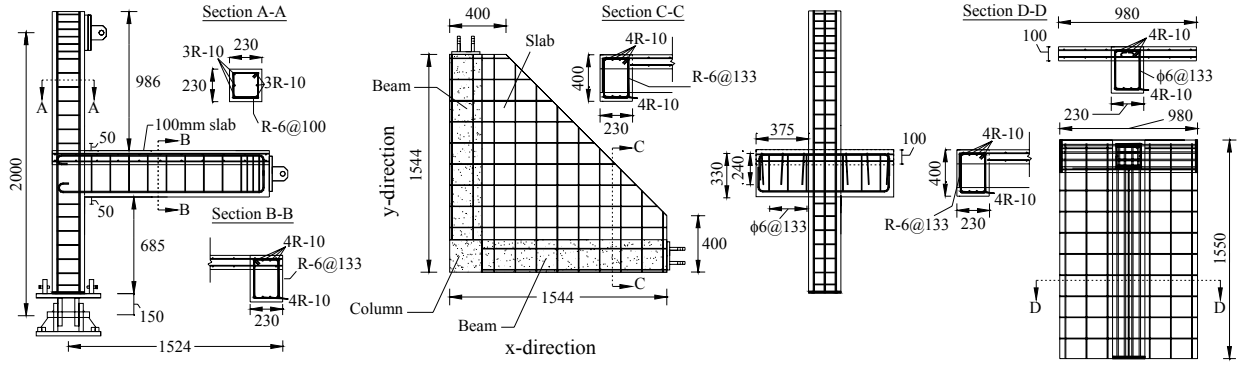

a) Beam-Column Joint Side View b) 3D-S slab plan view c) 2D-S column face elevation d) 2D-S plan view

Figure 1. Geometry and reinforcement details

Test setup and loading protocol

Figure 2 illustrates the test set-up and loading protocol adopted. Beam and column elements were extended between points of contra-flexure (assumed to be at mid-span in the beams and at mid-height in the columns) where pin connections were introduced. Simple supports at the beam ends were obtained connecting pin-end steel members to the strong floor. In general, the testing loading protocol consisted of increased level of lateral top displacements in each direction. More specifically, for the 3D configuration, in order to better simulate the actual displacement-imposed response under a real ground motion, a four clove loading protocol (Figure 2(b)) was adopted. It is worth noting that the two-cycle protocol used for the Y-direction component corresponds to the protocol adopted for the 2D b-c joints test.

In order to provide a more realistic representation of the behaviour of exterior b-c joints under uni- or bi-directional excitations, the axial load was varied as a function of the lateral force, F. The relationship between F and the variation of axial load N ($N= N_{gravity} \pm \alpha F$) is function of the geometry of the building (i.e. number of bays and storeys) and can be derived by simple hand calculations or pushover analyses on the prototype frame. Test were performed with $N_{gravity}$ = 110kN with coefficient α of 4.63 and 2.35 for 2D and 3D specimens respectively. For test unit 2D-S, a gravity loading corresponding to beam moment, $M_{b,initial\ g}$ = 10kNm and beam

shear, $V_{beam,initial}$ = 26kN was applied to impose realistic initial condition.

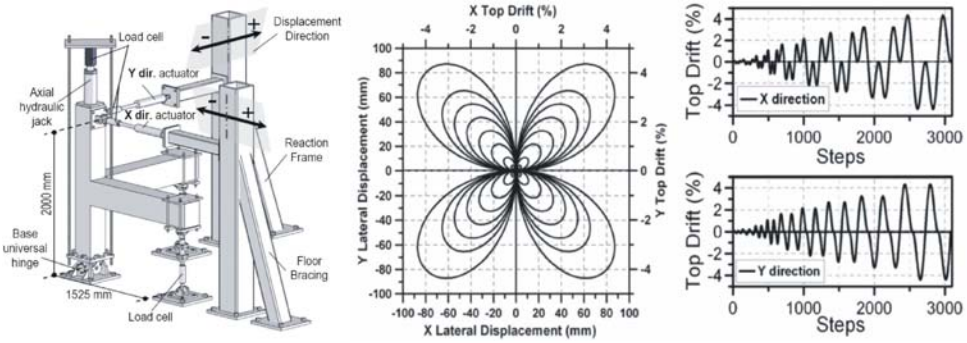

Figure 2. a) Experimental test set-up; (b) Four-cloves displacement loading protocol for uni- and bi-directional testing

One-way (2D) Exterior Beam-Column Joint Results

2D Benchmark specimen: 2D-B

The summary of the test results is presented in Table 2 and the force-displacement hysteresis responses of the four b-c joints are presented in Figure 3. All b-c joints were tested up to 3.0% cycles except for 2D-S, which did not 'fail' until the end of the 2nd cycles at 4.0% lateral drift. In general, both one-way (2D) test units exhibited joint shear failure – evident from damage observations (in Figure 4) and strain gages / potentiometers data.

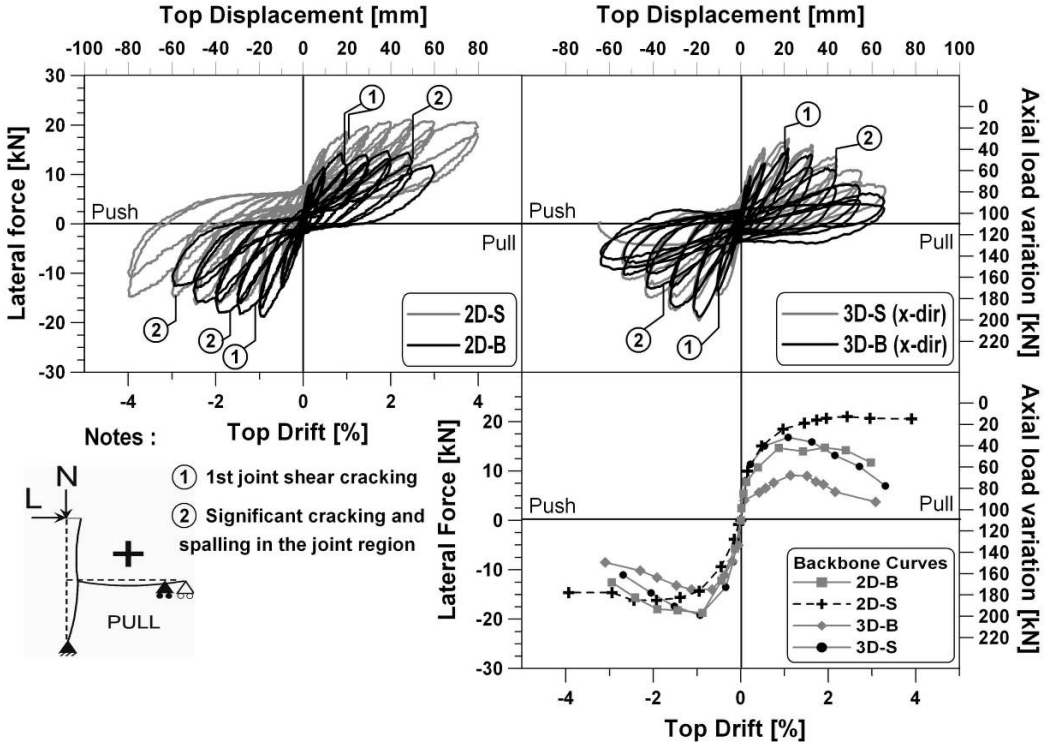

Figure 3. Experimental force-displacement hysteresis curves (1kN = 0.22482kips)

2D-B initially had some beam flexural cracks before developing a diagonal joint shear

crack at approximately 1st cycle peak of the 1.0% drift. Subsequent loading cycles further widened and extended the diagonal crack, leading to significant strength degradation and subsequently ultimate failure at the 2nd cycle of the 1.0% drift for 2D-B. The loss of bond along the beam reinforcements and ensuing push-out of the 180º degree beam bars anchorage resulted in a pinched hysteresis shape with limited energy dissipation. 2D-B ultimately lost its axial carrying capacity with column longitudinal bars buckling.

Table 1. Summary of experimental test results

Specimen	f_c`	Peak lateral force (kN)				Inter-storey drift at maximum force (%)				Ultimate inter-storey drift[c] (%)
		x direction		y direction		x direction		y direction		
	MPa	Pull	Push	Pull	Push	Pull	Push	Pull	Push	
2D-B	17.3	14.9	18.9	-	-	1.9	1.0	-	-	1[d] (pull dir.)
2D-S	13.4[a] 19.9[b]	21.2	16.3	-	-	2.4	2.4	-	-	3[d] (push dir.)
3D-B	17.4	15.3	18.8	13.6	18.3	1.1	1.0	1.1	0.7	1[d] (x-push dir./y-pull.dir)
3D-S	32.1[a] 26.2[b]	16.7	19.5	13.23	17.8	1.1	1.0	1.6	1.0	0.5[d] (x-pull dir./y-pull.dir)

[a,b]Compressive strength of concrete at the day of test for the upper column, and for the slab and lower column, respectively;
[c]Failure point defined as attained peak force is less than 80% of previous peak force;[d]Second loading cycle

2D benchmark with slab and transverse beam stubs: 2D-S

With transverse beam stubs, the cracking in the joint region could not be observed directed, but was deducted from indirect measurements (force-displacement, potentiometers and observable cracks). As seen in Figure 4b and c, it was evident that the un-reinforced joint region was damaged under joint shear cracking. Post-experiment forensic inspection revealed similar diagonal cracking within the joint region. However, the role of the slab in inducing torsion twist in the transverse beam, which subsequently added confinement to the joint, was apparent. Torsion cracks at approximately 54° inclination were observed on the transverse beam, consistent with previous experimental tests on exterior joints with slab and transverse beams (Durrani et al, 1987, Di Franco et al, 1995).

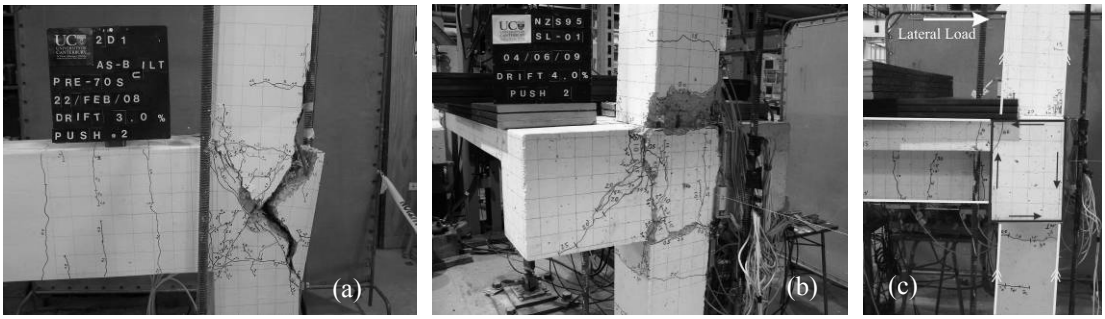

Figure 4. Failure pattern of two-dimensional specimens at the end of the tests: (a) 3D; (b) 3D-S; and c) deformed beam-column joint 3D-S at 3.0% Push cycle.

An evaluation of the subassembly force-displacement curves in Figure 3 shows an improved performance for 2D-S with higher lateral load and displacement capacity when compared to 2D-B. The higher displacement capacity can mostly be attributed to the torsion-

induced confinement from the transverse beam on the joint (see Figure 6). Meanwhile the higher lateral capacity was naturally from the slab tension flange effect for the negative moment capacity of the beam. However, lateral force was higher in the Pull direction (tension at bottom beam face) compared to the Push direction in 2D-S because of the gravity-loading imposed initial condition ($M_{b,initial}$= 10kNm) which effectively pre-compressed the bottom face of the beam.

However, as the inelastic mechanism was predominantly joint shear hinging in 2D-S, albeit a 'stable' hysteresis up to 3.0% drift cycles, plain-round bars bond slip and shear crack propagation resulted in a pinching low-energy-dissipation hysteresis for 2D-S. Evidently, the area-based equivalent viscous damping ratio for 2D-S and 2D-B were both similar, at approximately 10% in the first cycles and 6% in the 2nd cycles.

Floor slab and transverse beams on exterior 2D joint

In considering the influence of floor slab on the seismic behaviour of exterior 2D b-c joint, the contribution from the transverse (spandrel) beams must also be considered. A torsionally stiff transverse beam would result in large slab participation area within the tension flange near the b-c connection. Conversely, a weak and flexible transverse beam would result in smaller participation area – therefore smaller effective beam width (for flange effect. Consider the strain gage readings for all the Push (tension on beam top face) peaks within the 2D-S specimen, presented in Figure 5, with beam top longitudinal bars strain gages readings corresponding to the similar region. While tension strains were anticipated for the slab mesh, as it were for 2D-B longitudinal beam bars, the mesh just outside of the transverse beam were surprisingly in compression.

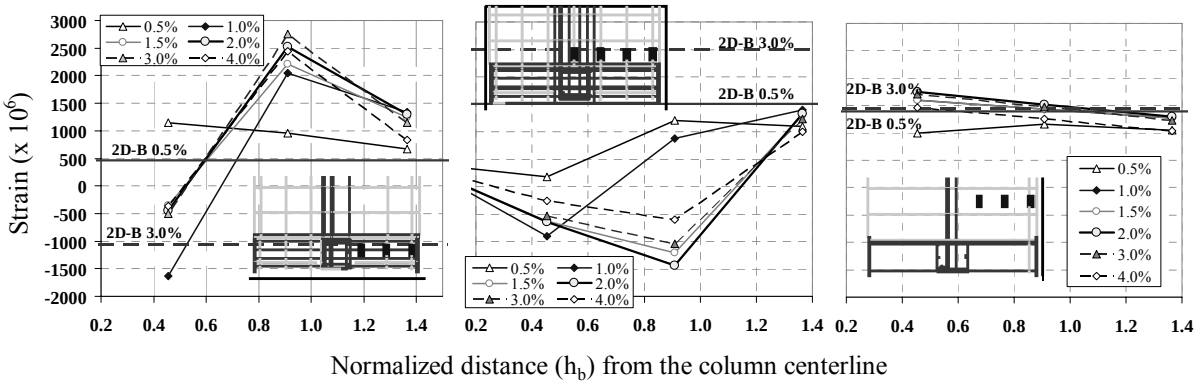

Figure 5. Strain gages readings for 2D-B and 2D-S at the Push direction peaks: row 1, 2 and 3.

The strain gages readings deviation between 2D-B and 2D-S can be explained using a strut-and-tie visualization of the transverse beam contribution, as given in Figure 6. Corresponding to the strain gages reading given in Figure 5, the increased tension strain in row 1 was possibly due to the tension chord activated by the torsion of the transverse beam. Similarly, the compressive strains in 2D-S, compared to tension strains in 2D-B, in row 2, was clear illustration of the compression strut shown in Figure 6. Lastly, in row 3 (~470mm from edge of slab)– there was no discrepancy between 2D-B and 2D-S strain gages reading, as transverse beam was no longer influencing the slab behaviour.

While not many bars of the slab mesh were yielding, from Figure 5, the participating slab

width for exterior b-c joints can be determined by the portion of slab that was affected by the torsion-induce flange effect as discussed by the preceding paragraph. At 2.0% drift, approximately $1.1h_b$ width of the slab was participating, based. This was relatively lower than previous tests with deformed bars (e.g. (Durrani et al, 1987))– as cracking in plain-round bars specimen typically concentrated in few discrete location – in 2D-S case – just outside the transverse beam region. This explains for the spike in strain readings at the strain gages located at $0.9h_b$ from the column center-line.

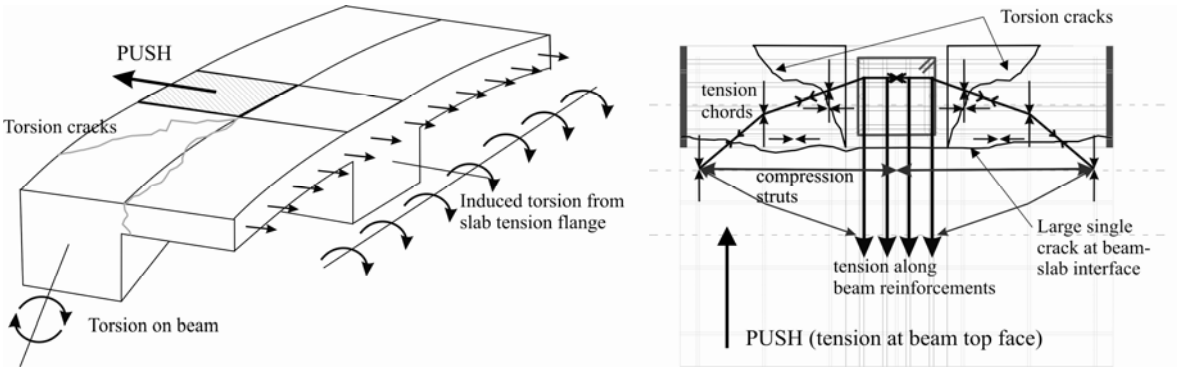

Figure 6. Role of transverse beams and slab on 2D exterior beam-column joint.

Two-way (3D) Exterior Beam-Column Joint Results

3D Benchmark specimen: 3D-B

The 3D specimen (3D1) exhibited a complex 3D concrete wedge mechanism (Figure 7a and b) due to the bi-directional loading regime confirming the damage observed in recent earthquakes. Similar to the 2D response, the first diagonal joint crack occurred at 1% of drift. A reduction in the overall load capacity of 33% and 15% in the positive and negative directions, respectively, was observed. Extensive joint damage and more strength degradation were observed compared to the 2D equivalent counterpart in spite of the partial confinement effect provided by the orthogonal beam. Higher level of damage and rapid strength degradation were observed in the 3D configurations subjected to bi-directional loading and (higher) variation of axial load, in spite of the partial confinement effect provided by the orthogonal beam.

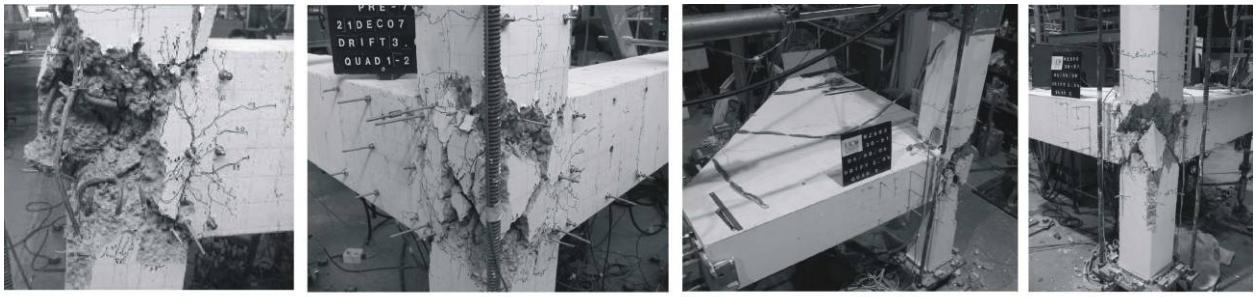

a) b) c) d)

Figure 7. Failure pattern of three-dimensional specimens at the end of the tests: (a) and (b) 3D; (c) and (d) 3D-S

3D specimen with slab: 3D-S

Test results of the current study indicated that the slab has a negligible influence on the global behavior in terms of bearing capacity only in both directions. As seen in the hysteresis loops (Fig. 3) and the final state of the specimen (Fig. 7c and d), brittle damage mechanisms were developed which are characterized by severe degradation in stiffness, pinching and loss of strength. Similar history in the formation and propagation of the damage were also observed in the counterpart test of specimen 3D-B. Typical flexural cracks around the b-c joint and slab interface have been noted at 0.5% drift with a maximum width of 0.6mm. First joint shear cracking was observed at 1% drift and followed by some longitudinal crack formation on the slab parallel to the beams axes in both directions. In the following cycles, these cracks were stabilized and new minor flexural cracks were developed under the beam faces. In general, after 1.5% drift level the behavior of the specimen was governed by extensive shear cracking followed by the initiation and spalling of the concrete wedge in the joint region which resulted in similar poor performance as observed in the specimen 3D.

Slab participation in 3D corner joint

As can be understood from the comparison of the load – displacement hysteretic loops of the 3D-B and 3D-S specimens, the slab has little influence in the overall performance of the subassembly. In Figure 8, the strain profile of the slab in the 3D-S specimen is presented. The results show that the slab reinforcement remained elastic during the test, with strains variations that follow the trend of the lateral shear capacity of the subassembly. The deformations in the slab at the end of the test are very similar than those reached at a 0.5% drift, indicating minor residual deformations which is in concordance with the small amount and width of cracks observed in the slab.

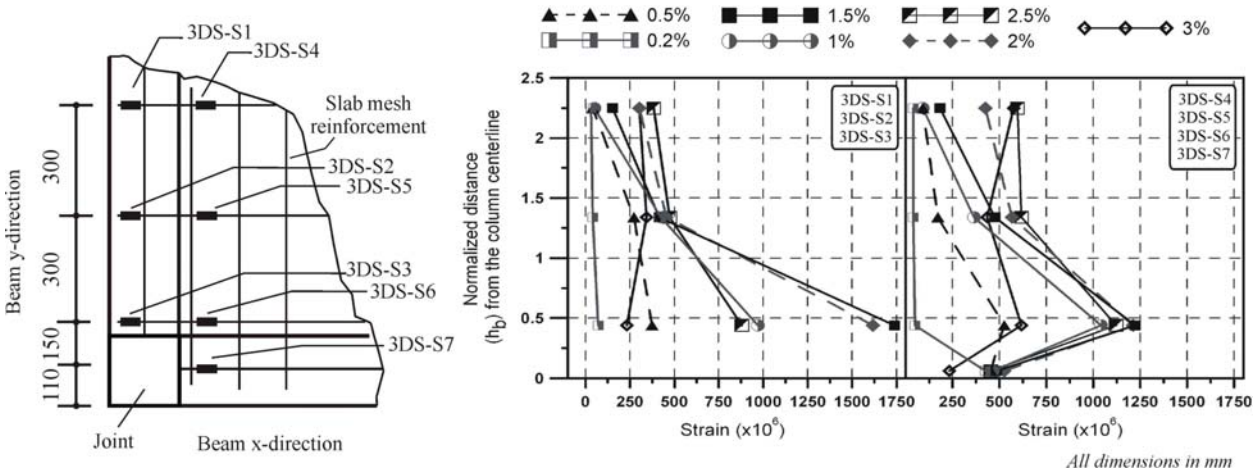

Figure 8. Strain gauge readings: left: strain profile in the slab inside the transverse beam; right: strain profile in the slab outside the transverse beam

In Figure 8, peak values of the strain gage readings in the slab reinforcement of specimen 3D-S are given for each drift level in the push loading direction, which caused tension in slab reinforcement and corresponds to the negative flexural moment in the beam. Examination of the

strain gage readings suggests that the reinforcement on the entire width of the slab did not equally participate in resisting the external moment, with higher strain levels near the beam interface. In general, strain readings in the transverse beam and slab showed similar trends up to 1% drift level. After 1.5% drift due to the accumulation of the damage in the joint region deformation demand is greatly reduced in the slab resulting in a decreasing level of strains up to the final state corresponding to 3% drift level. Strain readings in the mesh longitudinal bars in transverse beam (i.e. 3DS-S1, 3DS-S2) and slab (i.e. 3DS-S4, 3DS-S5) exhibited similar uniform trend with slightly large strain values at the outside transverse beam. It can also be seen in Figure 8 that the strain level on 3DS-S7 remains almost constant. This is attributed to loss of bond since that bar was not anchored in the column.

Considerations on slab-participation in non-ductile exterior beam-column joints

The experimental values for the effective flange width were derived from the reading of the strain-gages on the top mesh of the slabs. Typically the effective width of the slab is calculated considering the portion of the slab in which the bars are beyond the yielding strain at a fixed level of drift, usually 2% (French et al, 1991). However, as the joint-failure precluded mesh yielding in the 3D-S specimen, slab participation in the tension-flange has to be estimated using an approximate approach where the strains remain in the elastic range. From the strain readings in the flange, it can be seen that the mesh reinforcement is activated to a maximum level of strain that corresponds to 1.5% drift and then decays to an approximate constant level which can be attributed to self weight.

Consequently, the effective width of the slab is less than what can be expected in well designed structures, were premature failure in the joint is not observed, and where the strains in the slab keep on increasing with increasing drift levels. The use of plain round bars and poor anchorage of the reinforcement in the beam, leads to loss of bond between the reinforcement and the concrete, yielding typically one concentrated wide crack at the b-c interface. Also, the severe bi-directional seismic simulated loading increases this effect, preventing the slab to contribute much to the negative capacity of the beam, leading to a similar behavior of the subassembly when compared to the 3D-B specimen. In the case of 2D-S specimen, due to the presence of the transverse beam that provides confinement to the joint and torsional resistance, and due to the less severe loading protocol, the slab is activated beyond the yielding strain before severe damage is reached in the joint. Nevertheless, the strain level was well below that reached in test of well-designed subassemblies (Cheung et al, 1991).

Calculated effective width

The effective width of the slab (b_{eff}) measured in both 2D-S and 3D-S specimens are compared with the corresponding theoretical values given in ASCE-41(2007) and the NZSEE Seismic Assessment Guidelines (NZSEE, 2006). According to ASCE-41, the effective width of the slab must be calculated adding a portion of the slab on each side of the web of the beam equal to the lesser of (1) the provided flange width, (2) 8 times the slab thickness, (3) half the distance to the next web, and (4) 1/5 of the beam span. In the New Zealand normative, at each side of the beam centerline a value corresponding to the lesser of (1) 1/4 of the beam span, (2) 1/2 of the span of the slab transverse to the beam under consideration, and (3) 1/4 of the span of the transverse edge beam, must be considered. In Table 2 the experimental and theoretical values

according to the aforementioned normative are presented.

Table 2. Comparison of effective flange width between experimental results, ASCE-41 (2007) and NZSEE Seismic Assessment Guidelines (NZSEE, 2006).

Specimen	ASCE-SEI-41 (mm)	NZSEE (mm)	Experimental (mm)
2D-S	980 ($2.97h_b$)	1730 ($5.24h_b$)	726 ($2.20h_b$)
3D-S	830 ($2.52h_b$)	980 ($2.97h_b$)	700 ($2.12h_b$)

Based on this limited experimental results, it could be proposed that for seismic assessment of non-ductile exterior b-c joints, a minimum of approximately 2.2 times the beam depth ($2.2h_b$) is taken to be the effective flange width when calculating the beam negative moment. This would ensure a lower bound approximation for slab flange contribution when assessing hierarchy of strength (for capacity design consideration), while gives an lower bound in terms of beam negative flexural capacity. This is contrary to the common 'design' misconception where it is more conservative to adopt no flange contribution, whereas for assessment, it is more important to give an accurate representation of the b-c-joint hierarchy of strength.

This conclusion is consistent with some of the previous research suggesting slab participation based on torsional resistance of the spandrel beams (Durrani et al, 1987, Di Franco et al, 1995). However, as discussed before, their experimental data were based on beam flexural-hinging joints with modern seismic detailing – which limits its application to the seismic assessment of non-ductile RC buildings.

Conclusions

The results of four 2/3-scaled one-way and two-way exterior b-c joints with and without slabs experimental tests have been presented. From the 2D tests, slab and transverse beam stubs increased the lateral capacity of the b-c subassemblies slab tension flange, induced torsion within the transverse beam and subsequently provided lateral confinement to the joint. For the b-c joint with plain round bars and non-ductile detailing, the effective flange width due to interaction with the slab is lower than those observed in b-c joint with deformed bars and ductile detailing.

According to the test results herein presented, it was observed that the slab have minimum influence on the global behaviour of the two-way corner joint subassembly From strain gauges readings, it was noted that the strains in the slab did not exceed the yield level. Slab bars' strain reached a maximum at intermediate drift levels and decayed after that to similar values to those at low drift levels at the end of the test. This is remarkably but expectedly different from what has been found in previous experiments based on well designed specimens. Based on these findings, a recommendation to evaluate the effective width of the slab in the assessment phase is proposed. It is clear that for the seismic performance assessment of sub-standard detailed b-c joint connections, it is critical to accurately establish the slab tension-flange contribution to the beam capacity as well as the influence of transverse beam on the b-c joint behaviour. They would in turn modify the internal hierarchy of strength and influence the selection and design of an appropriate retrofit solution. It is proposed that for seismic assessment of non-ductile exterior b-c joints, a minimum of 2.2 times beam depths ($2.2h_{beam}$) is taken to be the effective flange width in calculating the beam negative moment.

Acknowledgments

This research is part of NZ FRST-funded project "Retrofit Solutions for NZ" (FRST Contract UOAX0411) www.retrofitsolutions.org.nz. Special thanks to Mr Mosese Fifita, who assisted in the construction and testing of the specimens.

References

ACI318-63. *Building code requirements for reinforced concrete (ACI318-63)*. Detroit: American Concrete Institute; 1963.

ASCE-SEI-41-06. Seismic rehabilitation of existing buildings. Reston, Va.: ASCE/SEI; 2007.

Aycardi LE, Mander JB, Reinhorn AM. Seismic resistance of R.C. frame structures designed only for gravity loads: Experimental performance of subassemblages. *ACI Structural Journal*. 1994;**91**(5):552-63.

Beres A, Pessiki S, White R, Gergely P. Implications of experimental on the seismic behaviour of gravity load designed RC beam-column connections. *Earthquake Spectra*. 1996;**12**(2):185-98.

Cheung PC, Paulay T, Park R. Mechanisms of slab contributions in beam-column subassemblages. In: Jirsa JO, editor. *Design of beam-column joints for seismic resistance, SP-123*. Detroit, MI: American Concrete Institute (ACI); 1991. p. 259-90.

Di Franco MA, Mitchell D, Paultre P. Role of spandrel beams on response of slab-beam-column connections. *ASCE J of Struct Eng*. 1995;**121**(3):408-19.

Durrani AJ, Zerbe HE. Seismic resistance of R/C exterior connections with floor slab. *ACI Structural Journal*. 1987;**113**(8):1850-64.

Ehsani MR, Wight J. Effect of transverse beams and slab on behaviour of reinforced concrete beam-to-column connections. *ACI Structural Journal*. 1985 Mar-Apr 195;**82**(2):188-95.

French CW, Moehle JP. Effect of floor-slab on behaviour of slab-beam-column connections. In: Jirsa JO, editor. *Design of beam-column joints for seismic resistance, SP-123*. Detroit, MI: American Concrete Institute; 1991. p. 225-58.

NZS95:1955. *New Zealand Standard - Model Building By-Laws: Part IV and V*. Wellington, New Zealand: New Zealand Standard Institute; 1955.

NZSEE. *Assessment and improvement of the structural performance of buildings in earthquakes*. Wellington, New Zealand: New Zealand Society for Earthquake Engineering (NZSEE); 2006.

Pampanin S, Calvi GM, Moratti M. Seismic behaviour of RC beam-column joints designed for gravity loads. *Proc. of 12th European Conference on Earthquake Eng*; 2002; London, UK, Paper 726, 2002.

Park R. A summary of result of simulated seismic load tests on reinforced concrete beam-column joints, beams and columns with substandard reinforcing details. *J of Earthquake Eng*. 2002;**6**(2):147-74.